

Abstract

An evaluation of the Cavity Attenuated Phase Shift particle light extinction monitor (CAPS PM_{ex}) by means of a combination of a 3-wavelength Integrating Nephelometer (NEPH; TSI Model 3563) and a 3-wavelength filter-based Particle Soot Absorption Photometer (PSAP) was carried out using both laboratory generated test particles and ambient aerosols. An accurate determination of a fixed pathlength correction for the CAPS PM_{ex} was made by comparing extinction measurements using polystyrene latex (PSL) spheres in combination with Mie scattering calculations to account for the presence of PSL conglomerates. These studies yielded a linear instrument response over the investigated dynamical range from 20 to 450 $M m^{-1}$ ($10^{-6} m^{-1}$) with a linear correlation coefficient of $R^2 > 0.98$. The adjustment factor was determined to be 1.05 times that previously reported. Correlating CAPS extinction to extinction measured by the NEPH-PSAP combination using laboratory-generated polydisperse mixtures of purely scattering ammonium sulfate and highly absorbing black carbon provided a linear regression line with slope $m = 0.99$ ($R^2 = 0.996$) for single-scattering albedo values ($\lambda = 630$ nm) ranging from 0.35 (black carbon) to 1.00 (ammonium sulfate). For ambient aerosol, light extinction measured by CAPS PM_{ex} was highly correlated ($R^2 = 0.995$) to extinction measured by the NEPH-PSAP combination with slope $m = 0.95$.

1 Introduction

The in situ measurement of atmospheric aerosol optical properties is an important component of quantifying climate change (IPCC, 2007; Schwartz et al., 2010). In particular, in-situ measurement of the aerosol single-scattering albedo (SSA), which is the ratio of aerosol scattering to aerosol extinction, is identified as a key challenge in atmospheric sciences and climate change research (Loeb and Su, 2010). Ideally, the complete set of aerosol optical properties is measured through optical closure studies which simultaneously measure aerosol extinction, scattering and absorption coefficients. The recent

Intercomparison of CAPS PM_{ex} with an Integrating Nephelometer/PSAP

A. Petzold et al.

Title Page

Abstract

Introduction

Conclusions

References

Tables

Figures

◀

▶

◀

▶

Back

Close

Full Screen / Esc

Printer-friendly Version

Interactive Discussion

**Intercomparison of
CAPS PM_{ex} with an
Integrating
Nephelometer/PSAP**A. Petzold et al.

[Title Page](#)[Abstract](#)[Introduction](#)[Conclusions](#)[References](#)[Tables](#)[Figures](#)[⏪](#)[⏩](#)[◀](#)[▶](#)[Back](#)[Close](#)[Full Screen / Esc](#)[Printer-friendly Version](#)[Interactive Discussion](#)

development of new optical instruments has made real-time in situ optical closure studies attainable, including from mobile platforms such as aircraft (Langridge et al., 2011); however, many of these instruments are state-of-the-art and not practical for routine monitoring. Here, we evaluate the recently developed Cavity Attenuated Phase Shift particle light extinction monitor (CAPS PM_{ex}) against current standard techniques for routine monitoring of aerosol optical properties.

Aerosol extinction, scattering and absorption coefficients are measured using different techniques. The particle scattering coefficient σ_{sp} is typically measured by an Integrating Nephelometer (Heintzenberg et al., 2006). For the particle absorption coefficient, σ_{ap} , either filter-based or in-situ methods are available, both of which have been extensively investigated in various studies (Arnott et al., 2003; Sheridan et al., 2005; Müller et al., 2011). In the laboratory, the direct measurement of the particle extinction coefficient σ_{ep} is performed with long-path extinction cells (Schnaiter et al., 2005) or cavity ring-down systems (Strawa et al., 2003), while various methods exist for atmospheric measurements (Schmid et al., 2006).

Long-path extinction cells are limited in their lower detection range to extinction coefficients well above 10 Mm^{-1} ; e.g. both Schnaiter et al. (2005) and Chartier and Greenslade (2012) report for their long-path extinction spectrometers noise levels of 20 Mm^{-1} for extinction cells of optical path length of 10 m and ~ 20 m, respectively for integration times of several minutes. According to the underlying Lambert–Beer law, an improvement of the lower detection limit can be achieved only by increasing the optical path length which, however, imposes geometrical limitations. In contrast to long-path extinction cells, the Cavity Ring-Down (CRD) method yields the aerosol extinction coefficient by measuring the time constant for light decay in a high-finesse cavity containing the absorbing and scattering particles. A detailed introduction to the CRD technique for aerosol extinction measurement is given by Strawa et al. (2003) whereas Moosmüller et al. (2005) provide an overview over the various CRD and cavity-enhanced detection approaches. Driven by a rapid technology development, CRD instruments are now available as multi-wavelength systems for atmospheric measurements (Atkinson et al.,

2010; Schmid et al., 2006) and laboratory studies (Butler et al., 2009; Cross et al., 2010; Sheridan et al., 2005).

5 Recently, a compact and robust family of optical instruments based on the cavity attenuated phase shift technique has become available (Kebabian et al., 2007). In particular, the CAPS PM_{ex} particle optical extinction monitor has demonstrated sensitivity (2 s) of less than 2 Mm⁻¹ in 1 s sampling period; with a 60 s averaging time, a detection limit of less than 0.3 Mm⁻¹ can be achieved. The CAPS PM_{ex} technique, similar in its basic principle to cavity ring-down, relies on the use of a short (26 cm) sample cell employing high reflectivity mirrors (Kebabian and Freedman, 2007; Kebabian et al., 2007). Square-wave modulated light emitted from a light emitting diode (LED) at a wavelength ~ 630 nm is directed through one mirror into the sample cell. The distortion in the square wave caused by the effective optical path length within the cavity (approx. 2 km light path) is measured as a phase shift in the signal as detected by a vacuum photodiode which is located behind the second mirror. A detailed description of the method including first results from laboratory characterization and field deployment is given by Massoli et al. (2010), while Yu e al. (2011) reports an application to the direct measurement of combustion particle emissions from aircraft engines.

15 This study characterizes the CAPS PM_{ex} instrument for both laboratory test aerosols and ambient aerosol. The CAPS PM_{ex} instrument was evaluated against a combination of an Integrating Nephelometer (NEPH; TSI Model 3563), a particle soot absorption photometer (PSAP; Radiance Research) (Virkkula et al., 2005) and a Multi-Angle Absorption Photometer (MAAP) (Petzold and Schönlinner, 2004; Petzold et al., 2005).

20 The experimental approach taken for the evaluation of the CAPS PM_{ex} extinction monitor was divided into three consecutive steps: (1) an accurate determination of instrument pathlength adjustment by using non-absorbing PSL spheres combined with Mie theory calculations; (2) instrument intercomparison with polydisperse laboratory aerosols of known composition; and (3) instrument intercomparison for ambient aerosol.

Intercomparison of CAPS PM_{ex} with an Integrating Nephelometer/PSAP

A. Petzold et al.

Title Page

Abstract

Introduction

Conclusions

References

Tables

Figures



Back

Close

Full Screen / Esc

Printer-friendly Version

Interactive Discussion



2 Experimental section

2.1 Instrumental set-up

Instruments deployed in our study were the CAPS PM_{ex} extinction monitor for measuring the particle extinction coefficient, σ_{ep} , the PSAP and MAAP instruments for measuring the particle absorption coefficient, σ_{ap} , and a NEPH for measuring the particle scattering coefficient, σ_{sp} . Instrument details and acronyms used in this publication are summarized in Table 1.

Monodisperse particle distributions of PSL spheres (Duke Scientific Corp., Palo Alto, CA) of nominal sizes 350 ± 7 nm, 499 ± 5 nm, 596 ± 6 nm, 701 ± 6 nm, and 903 ± 9 nm were nebulized in a Collison-type atomizer (Massoli et al., 2010), dried to $\leq 25\%$ relative humidity (RH) in a tube filled with silica gel, size-selected by a differential mobility analyzer and fed into the CAPS PM_{ex} extinction monitor. The total number concentration, N_{total} , and the size distribution of the PSL spheres were measured simultaneously by an optical particle counter (OPC) (Grimm Model 1.129) which has a lower detection size limit of 250 nm in diameter for a particle refractive index of 1.585. The experimental set-up used for the instrument calibration is shown in Fig. 1.

Polydisperse test aerosols were generated in a laboratory setting with varying SSA values ranging from 0.35 to 1.0 at a wavelength of 630 nm by mixing purely scattering ammonium sulfate (AS) particles with strongly absorbing black carbon (BC) aerosol (Regal 400R pigment black, Cabot Corp.). Both types of aerosols were generated by nebulizing a solution of the respective substance in deionized water in an atomizer and drying the aerosol as described above. When generating external aerosol mixtures, the pure aerosols were fed into a 3I-mixing volume where the instruments sampled from. Particle-free make-up air was added downstream of the mixing volume to balance the input flow from the atomizers and the overall flow sampled by the instruments. The set-up used for the polydisperse laboratory aerosol studies is shown schematically in Fig. 2.

Intercomparison of CAPS PM_{ex} with an Integrating Nephelometer/PSAP

A. Petzold et al.

Title Page

Abstract

Introduction

Conclusions

References

Tables

Figures

⏪

⏩

◀

▶

Back

Close

Full Screen / Esc

Printer-friendly Version

Interactive Discussion



Intercomparison of CAPS PM_{ex} with an Integrating Nephelometer/PSAP

A. Petzold et al.

Title Page

Abstract

Introduction

Conclusions

References

Tables

Figures

⏪

⏩

◀

▶

Back

Close

Full Screen / Esc

Printer-friendly Version

Interactive Discussion



correction schemes are based on the measured light scattering Ångström exponent $\alpha_{sp} = -\log(\sigma_{sp,450}/\sigma_{sp,700})/\log(450/700)$; see Massoli et al. (2009) for details.

The PSAP raw signal was corrected according to Virkkula et al. (2005, 2010) and Ogren (2010) using the NEPH data. PSAP data measured at filter transmissions < 70 % were rejected, as recommended by Bond et al. (1999). MAAP and CAPS PM_{ex} data were used without further corrections except the adjustment to temperature and pressure measured by the NEPH, i.e. all data refer to same pressure and temperature conditions.

Data from CAPS PM_{ex} and from NEPH-PSAP were processed on the basis of the NEPH time resolution of 10 s, whereas MAAP data are reported on a 1 min time resolution. For the final evaluation of instrument performances for ambient aerosol, all instrument data were converted to 10 min time averages.

For instrument intercomparison purposes, all instruments were adjusted to the wavelength of 630 nm. Data were compared in the red spectral region since both single-wavelength instruments, CAPS PM_{ex} and MAAP, operate at $\lambda \cong 630$ nm and the 3-wavelength instruments, NEPH and PSAP, allow for a wavelength-dependent adjustment based on direct measurement. For the sake of data robustness, PSAP data for σ_{ap} were scaled according to the λ^{-1} scaling law (Bohren and Huffman, 1983) while NEPH data for σ_{sp} were adjusted by applying the measured scattering Ångström exponent. Figure 3 summarizes the data inversion schemes applied to the various instruments.

3 Results

3.1 Determination of pathlength adjustment

The CAPS PM_{ex} extinction monitor provides an absolute measurement of particle light extinction. However, in order to keep the mirrors from being contaminated by the particles, a small volume in front of each mirror must be flooded with particle-free purge gas, thus shortening the effective pathlength. As noted in Massoli et al. (2010), this

effect was approximately measured using nitrogen dioxide, an absorbing gas. When extinction measurements using PSL spheres were compared to Mie scattering cross sections calculated assuming a monodisperse size distribution, the results were within the $\pm 10\%$ uncertainty of the condensation particle counter used to measure particle concentration.

In the present study, we measured the pathlength adjustment using PSL particles and Mie theory. The actual PSL size distributions were measured by means of an optical particle counter. The measured size distributions were parameterized as bi-modal log-normal size distributions which then served as input to the Mie code. The number concentrations of the two log-normal modes $N(\text{mode 1})$ and $N(\text{mode 2})$ were normalized to N_{total} so that $N_1 + N_2 = 1$ with $N_1 = N(\text{mode 1})/N_{\text{total}}$ and $N_2 = N(\text{mode 2})/N_{\text{total}}$. Single-particle extinction cross-sections for the polydisperse case were then calculated as $C_{\text{ext, poly}} = N_1 \times C_{\text{ext}}(d_{g1}, \sigma_{g1}) + N_2 \times C_{\text{ext}}(d_{g2}, \sigma_{g2})$. The PSL extinction coefficients were calculated using the BHMIE code (Bohren and Huffman, 1983) for $\lambda = 630 \text{ nm}$ and a refractive index of $1.585 + 0.0i$. Finally, the extinction coefficient $\sigma_{\text{ep, poly}}$ was obtained by $\sigma_{\text{ep, poly}} = N_{\text{total}} \times C_{\text{ext, poly}}$. Calculating the extinction coefficient of the polydisperse aerosol from normalized size distributions has the advantage of a direct comparison of extinction cross-sections for monodisperse and polydisperse calibration aerosols which provides a measure for the uncertainty introduced into the calibration procedure by the simplified assumption of single-sized PSL spheres.

Figure 4 shows number size distributions measured for the indicated PSL standards. Although the size distributions are dominated by the nominal PSL sphere mode, PSL conglomerates were observed. Input data to the Mie calculations and results of the instrument calibration are compiled in Table 2. Calculated values for $C_{\text{ext, mono}}$ and $C_{\text{ext, poly}}$ deviate by -8.33% (350 nm), 3.41% (499 nm), -1.82% (596 nm), 23.40% (701 nm), and 6.80% (903 nm), i.e. the simplified and the advanced approach show no systematic differences, though they differ statistically.

Correlation plots comparing extinction as calculated by Mie theory and extinction as measured by CAPS PM_{ex} are shown in Fig. 5. CAPS PM_{ex} data were averaged over

Intercomparison of CAPS PM_{ex} with an Integrating Nephelometer/PSAP

A. Petzold et al.

Title Page

Abstract

Introduction

Conclusions

References

Tables

Figures

⏪

⏩

◀

▶

Back

Close

Full Screen / Esc

Printer-friendly Version

Interactive Discussion

Intercomparison of CAPS PM_{ex} with an Integrating Nephelometer/PSAP

A. Petzold et al.

Title Page

Abstract

Introduction

Conclusions

References

Tables

Figures

⏪

⏩

◀

▶

Back

Close

Full Screen / Esc

Printer-friendly Version

Interactive Discussion



3–5 min sequences after the aerosol generator output had stabilized sufficiently. The error bars in Fig. 5 correspond to 1- σ of the sequence average. Results of the respective linear regression analyses are inserted in the graphs. In both cases measured and calculated extinction coefficients are highly correlated with $R^2 > 0.98$. The slopes of regression lines are 0.96 (polydisperse) and 0.95 (monodisperse) with the differences being below statistical significance.

These PSL sphere experiments prove the excellent correlation between CAPS PM_{ex} extinction monitor response and calculated extinction coefficients. Both approaches of using either the nominal PSL sphere size and the total number concentration or the full size distribution information for calculating the expected extinction coefficients agree well. These results indicate that the original gas phase-based pathlength adjustment measurement, included in the CAPS PM_{ex} data acquisition software, was low by 5%. The current pathlength adjustment measurement agrees with the pathlength adjustment estimated from instrument geometry. As a consequence, CAPS PM_{ex} data for the instrument evaluation using laboratory generated polydisperse test aerosols and for the intercomparison purposes based on ambient aerosol data were corrected for the new pathlength adjustment by multiplication with a factor of 1.05.

3.2 Instrument evaluation using test aerosols

As an illustration of the laboratory intercomparison studies, Fig. 6 shows a time series of the extinction coefficients measured during the AS-BC test aerosol runs. A similar time series exists for pure AS aerosol which, however, is not shown here. The analysis of the CAPS PM_{ex} data and the combined NEPH-PSAP data was restricted to sequences of stable aerosol concentrations. Table 3 compiles the data obtained from the averaging sequences of the various test aerosols. As indicated by the single-scattering albedo (SSA) values listed in Table 3, the instrument evaluation covered the entire SSA range from 0.35 to 1.00 with test points at 0.81, 0.89, and 0.96. Thus, the entire SSA range relevant for ambient aerosol measurements is covered by the generated test aerosols.

Intercomparison of CAPS PM_{ex} with an Integrating Nephelometer/PSAP

A. Petzold et al.

Title Page

Abstract

Introduction

Conclusions

References

Tables

Figures

⏪

⏩

◀

▶

Back

Close

Full Screen / Esc

Printer-friendly Version

Interactive Discussion



The ratio of σ_{ep} (CAPS PM_{ex}) to σ_{ep} (NEPH-PSAP) is listed in the rightmost column of Table 3. Due to the limited number of data points we analyzed the median instead of mean values for the respective test aerosols and obtained 1.09 for AS, 0.94 for BC, and 0.97 for the mixed cases. For the entire set of 12 data pairs the median ratio is 0.997 while the respective mean and 1- σ values of the distribution are 1.018 ± 0.074 .

Figure 7a displays the instrument evaluation data set graphically demonstrating the excellent accuracy of the CAPS PM_{ex} instrument determined by comparison to the NEPH-PSAP combination. Linear regression analysis of the entire data set ($n = 12$) yields a slope $m = 1.005 \pm 0.025$ if the zero intercept is set to 0.0, and $m = 1.002 \pm 0.02$ with zero intercept $a = 1.44 \pm 7.26$. For both cases the correlation coefficient $R^2 > 0.99$. Figure 7b shows a correlation plot of data obtained from two different CAPS PM_{ex} monitors (operating at 530 nm), both of which sampled ambient air from a common inlet. The least squares fit to this data yield a slope of 1.00 ± 0.01 with zero intercept $a = 0.17 \pm 0.01$ and $R^2 = 0.990$ which provides an indication of the repeatability of the CAPS PM_{ex} monitors. This level of agreement is comparable to that obtained using a monochromatic laser-based cavity ringdown system (Massoli et al., 2010).

The relative precision of the CAPS PM_{ex} monitor and NEPH-PSAP combination is shown in Fig. 8 as the histogram of data reported by the instruments during 1h of sampling of particle-free air. The CAPS PM_{ex} instrument reports $\sigma_{ep,zero} = -0.25 \pm 0.91 \text{ Mm}^{-1}$ and -0.00 ± 0.19 on average for 1 s and 10 s data, respectively, in agreement with previous studies (Massoli et al., 2010). The NEPH-PSAP combination yields $\sigma_{ep,zero} = 0.47 \pm 0.47 \text{ Mm}^{-1}$ on average for 10 s data. The small offset is statistically insignificant.

3.3 Method intercomparison for ambient aerosol

The first week of a two-week period for sampling of ambient aerosol (27 May to 8 June 2011) was characterized by a hot and humid stagnant high-pressure situation with reduced air mass exchange and thus air pollution accumulation. During this initial

neither aerosol SSA nor relative humidity. An agreement of better than 95 % between these two methods can be rated as excellent. Similar results are reported from a recent study operating one CAPS PM_{ex} and a NEPH-PSAP combination in the Storm Peak Laboratory, USA (Andrews et al., 2012).

5 The ratio of CAPS PM_{ex} to NEPH-PSAP data is plotted in Fig. 12 for all investigated aerosol types. This graph illustrates an apparent discrepancy between the CAPS PM_{ex} and the NEPH-PSAP extinction measurements for ambient data; the CAPS PM_{ex} is approximately 5 % low compared to NEPH-PSAP, with the bulk of data falling in the range 0.90–1.05. More important, however, is the observation that the scatter in the
10 ratio σ_{ep} (CAPS PM_{ex})/ σ_{ep} (NEPH-PSAP) is not correlated to the absolute value of σ_{ep} which demonstrates the robustness of the CAPS PM_{ex} method compared to the current standard method of the NEPH-PSAP combination.

4 Discussion and conclusions

15 The results from the instrument calibration work with PSL spheres and Mie theory yield a strong correlation ($R^2 > 0.98$) between instrument response and light extinction calculated by Mie theory. The particle-based measurements indicate a pathlength adjustment of 1.05 compared to previous gas phase-based estimates. The new pathlength adjustment factor agrees with instrument geometry. With this one-time adjustment, the CAPS PM_{ex} technique appears to provide a very accurate measurement of aerosol
20 light extinction.

Instrument evaluation of CAPS PM_{ex} versus the NEPH-PSAP combination using highly absorbing black carbon particles (regal black), exclusively scattering aerosol (ammonium sulfate) and mixtures of both show excellent correlation between methods. The slope of the regression line is 0.99, demonstrating the robustness of the calibration
25 for aerosol particles with single scattering albedoes ranging from strongly absorbing with SSA = 0.35 to purely scattering with SSA = 1.0.

Intercomparison of CAPS PM_{ex} with an Integrating Nephelometer/PSAP

A. Petzold et al.

Title Page

Abstract

Introduction

Conclusions

References

Tables

Figures

⏪

⏩

◀

▶

Back

Close

Full Screen / Esc

Printer-friendly Version

Interactive Discussion



Intercomparison of CAPS PM_{ex} with an Integrating Nephelometer/PSAP

A. Petzold et al.

Title Page

Abstract

Introduction

Conclusions

References

Tables

Figures



Back

Close

Full Screen / Esc

Printer-friendly Version

Interactive Discussion



This instrument intercomparison between the CAPS PM_{ex} and the current standard combination of NEPH-PSAP for ambient aerosol sampled from a roof-top inlet serves as realistic test case for the measurement of ambient aerosol under field conditions. The bulk of the CAPS PM_{ex} data deviate from respective NEPH-PSAP data by -5% , indicating a small but robust disagreement which is not present for the laboratory studies. There are a number of possible explanations for this small level of disagreement. One possibility is particle loss in any of the instruments. Unlike the laboratory studies, the ambient measurements contained substantial contributions to scattering from supra-micron particles which are more likely to be lost in transfer. Another is that the truncation correction for the NEPH is more uncertain for particles of diameter greater than $1\ \mu\text{m}$, the largest diameter sampled in the laboratory studies. Relative humidity (which was not controlled in the ambient studies) does not appear to be an issue given that the ambient studies included periods of both very high and low RH.

Acknowledgement. This study was conducted during a research stay of A. Petzold at Aerodyne Research Inc. in 2011 when he was employed by Deutsches Zentrum für Luft- und Raumfahrt (DLR). The support of this stay by DLR is gratefully acknowledged. The authors thank A. Ibrahim (DLR) for his valuable contributions during the measurement periods. The provision of the PM₁₀ sampling head for the ambient aerosol sampling line by Thermo Fischer is gratefully acknowledged. The efforts of the Aerodyne personnel were supported by the US Department of Energy, NASA and the National Institutes of Health, all under the Small Business Innovation Research program.

The service charges for this open access publication have been covered by a Research Centre of the Helmholtz Association.

References

- Anderson, T. L., and Ogren, J. A.: Determining aerosol radiative properties using the tsi 3563 integrating nephelometer, *Aerosol Sci. Tech.*, 29, 57–69, 1998.
- Andrews, E., Massoli, P., Hallar, A. G., Sedlacek, A., Freedman, A., Ogren, J. A., and Sheridan, P.: Absorption closure – filter-based absorption instruments compared to extinction-scattering measurements, European Aerosol Conference, Granada Spain, 2–7 September 2012.
- Arnott, W. P., Moosmüller, H., Sheridan, P. J., Ogren, J. A., Raspert, R., Slaton, W. V., Hand, J. L., Kreidenweis, S. M., and Collett, J. L. J.: Photoacoustic and filter-based ambient aerosol light absorption measurements: instrument comparisons and the role of relative humidity, *J. Geophys. Res.*, 108, 4034, doi:10.1029/2002JD002165, 2003.
- Atkinson, D. B., Massoli, P., O’Neill, N. T., Quinn, P. K., Brooks, S. D., and Lefer, B.: Comparison of in situ and columnar aerosol spectral measurements during TexAQS-GoMACCS 2006: testing parameterizations for estimating aerosol fine mode properties, *Atmos. Chem. Phys.*, 10, 51–61, doi:10.5194/acp-10-51-2010, 2010.
- Bohren, C. F. and Huffman, D. R.: *Absorption and Scattering of Light by Small Particles*, John Wiley & Sons, Inc, New York, 544 pp., 1983.
- Bond, T. C., Anderson, T. L., and Campbell, D.: Calibration and intercomparison of filter-based measurements of visible light absorption by aerosols, *Aerosol Sci. Tech.*, 30, 582–600, 1999.
- Butler, T. J. A., Mellon, D., Kim, J., Litman, J., and Orr-Ewing, A. J.: Optical-feedback cavity ring-down spectroscopy measurements of extinction by aerosol particles, *J. Phys. Chem. A*, 113, 3963–3972, doi:10.1021/jp810310b, 2009.
- Chartier, R. T. and Greenslade, M. E.: Initial investigation of the wavelength dependence of optical properties measured with a new multi-pass aerosol extinction differential optical absorption spectrometer (AE-DOAS), *Atmos. Meas. Tech.*, 5, 709–721, doi:10.5194/amt-5-709-2012, 2012.
- Cross, E. S., Onasch, T. B., Ahern, A., Wrobel, W., Slowik, J. G., Olfert, J., Lack, D. A., Massoli, P., Cappa, C. D., Schwarz, J. P., Spackman, J. R., Fahey, D. W., Sedlacek, A., Trimborn, A., Jayne, J. T., Freedman, A., Williams, L. R., Ng, N. L., Mazzoleni, C., Dubey, M., Brem, B., Kok, G., Subramanian, R., Freitag, S., Clarke, A., Thornhill, D., Marr, L. C., Kolb, C. E., Worsnop, D. R., and Davidovits, P.: Soot particle studies-instrument intercomparison-project overview, *Aerosol Sci. Tech.*, 44, 592–611, 2010.

Intercomparison of CAPS PM_{ex} with an Integrating Nephelometer/PSAP

A. Petzold et al.

Title Page

Abstract

Introduction

Conclusions

References

Tables

Figures

⏪

⏩

◀

▶

Back

Close

Full Screen / Esc

Printer-friendly Version

Interactive Discussion



Intercomparison of CAPS PM_{ex} with an Integrating Nephelometer/PSAP

A. Petzold et al.

[Title Page](#)
[Abstract](#)
[Introduction](#)
[Conclusions](#)
[References](#)
[Tables](#)
[Figures](#)
[Back](#)
[Close](#)
[Full Screen / Esc](#)
[Printer-friendly Version](#)
[Interactive Discussion](#)


- Heintzenberg, J., Wiedensohler, A., Tuch, T. M., Covert, D. S., Sheridan, P., Ogren, J. A., Gras, J., Nessler, R., Kleefeld, C., Kalivitis, N., Aaltonen, V., Wilhelm, R. T., and Havlicek, M.: Intercomparisons and aerosol calibrations of 12 commercial integrating nephelometers of three manufacturers, *J. Atmos. Ocean. Tech.*, 23, 902–914, 2006.
- 5 IPCC: *Climate Change 2007: The Scientific Basis*, Cambridge University Press, Cambridge, 940 pp., 2007.
- Kebabian, P. L. and Freedman, A.: System and method for trace species detection using cavity attenuated phase shift spectroscopy with an incoherent light source, US Patent No. 7301639, issued 27 November 2007.
- 10 Kebabian, P. L., Robinson, W. A., and Freedman, A.: Optical extinction monitor using cw cavity enhanced detection, *Rev. Sci. Instrum.*, 78, 063102, doi:10.1063/1.2744223, 2007.
- Langridge, J. M., Richardson, M. S., Lack, D., Law, D., and Murphy, D. M.: Aircraft instrument for comprehensive characterization of aerosol optical properties, Part I: Wavelength-dependent optical extinction and its relative humidity dependence measured using cavity ringdown spectroscopy, *Aerosol Sci. Tech.*, 45, 1305–1318, doi:10.1080/02786826.2011.592745, 2011.
- 15 Loeb, N. G. and Su, W. Y.: Direct aerosol radiative forcing uncertainty based on a radiative perturbation analysis, *J. Climate*, 23, 5288–5293, doi:10.1175/2010jcli3543.1, 2010.
- Massoli, P., Murphy, D. M., Lack, D. A., Baynard, T., Brock, C. A., and Lovejoy, E. R.: Uncertainty in light scattering measurements by tsi nephelometer: Results from laboratory studies and implications for ambient measurements, *Aerosol Sci. Tech.*, 43, 1064–1074, 2009.
- 20 Massoli, P., Kebabian, P. L., Onasch, T. B., Hills, F. B., and Freedman, A.: Aerosol light extinction measurements by cavity attenuated phase shift (CAPS) spectroscopy: laboratory validation and field deployment of a compact aerosol particle extinction monitor, *Aerosol Sci. Tech.*, 44, 428–435, doi:10.1080/02786821003716599, 2010.
- 25 Moosmüller, H., Varma, R., and Arnott, W. P.: Cavity ring-down and cavity-enhanced detection techniques for the measurement of aerosol extinction, *Aerosol Sci. Tech.*, 39, 30–39, doi:10.1080/027868290903880, 2005.
- Müller, T., Henzing, J. S., de Leeuw, G., Wiedensohler, A., Alastuey, A., Angelov, H., Bizjak, M., Collaud Coen, M., Engström, J. E., Gruening, C., Hillamo, R., Hoffer, A., Imre, K., Ivanow, P., Jennings, G., Sun, J. Y., Kalivitis, N., Karlsson, H., Komppula, M., Laj, P., Li, S.-M., Lunder, C., Marinoni, A., Martins dos Santos, S., Moerman, M., Nowak, A., Ogren, J. A., Petzold, A., Pichon, J. M., Rodriguez, S., Sharma, S., Sheridan, P. J., Teinilä, K., Tuch, T., Viana, M., Virkkula, A., Weingartner, E., Wilhelm, R., and Wang, Y. Q.: Characterization
- 30

Intercomparison of CAPS PM_{ex} with an Integrating Nephelometer/PSAP

A. Petzold et al.

[Title Page](#)
[Abstract](#)
[Introduction](#)
[Conclusions](#)
[References](#)
[Tables](#)
[Figures](#)
[⏪](#)
[⏩](#)
[◀](#)
[▶](#)
[Back](#)
[Close](#)
[Full Screen / Esc](#)
[Printer-friendly Version](#)
[Interactive Discussion](#)


- and intercomparison of aerosol absorption photometers: result of two intercomparison workshops, *Atmos. Meas. Tech.*, 4, 245–268, doi:10.5194/amt-4-245-2011, 2011.
- Ogren, J. A.: Comment on “Calibration and intercomparison of filter-based measurements of visible light absorption by aerosols”, *Aerosol Sci. Tech.*, 44, 589–591, 2010.
- 5 Petzold, A. and Schönlinner, M.: Multi-angle absorption photometry – a new method for the measurement of aerosol light absorption and atmospheric black carbon, *J. Aerosol Sci.*, 35, 421–441, 2004.
- Petzold, A., Schlösser, H., Sheridan, P. J., Arnott, W. P., Ogren, J. A., and Virkkula, A.: Evaluation of multiangle absorption photometry for measuring aerosol light absorption, *Aerosol Sci. Tech.*, 39, 40–51, 2005.
- 10 Schmid, B., Ferrare, R., Flynn, C., Elleman, R., Covert, D., Strawa, A., Welton, E., Turner, D., Jonsson, H., Redemann, J., Eilers, J., Ricci, K., Hallar, A. G., Clayton, M., Michalsky, J., Smirnov, A., Holben, B., and Barnard, J.: How well do state-of-the-art techniques measuring the vertical profile of tropospheric aerosol extinction compare?, *J. Geophys. Res.-Atmos.*, 111, D05S07, doi:10.1029/2005jd005837, 2006.
- 15 Schnaiter, M., Schmid, O., Petzold, A., Fritzsche, L., Klein, K. F., Andreae, M. O., Helas, G., Thielmann, A., Gimmler, M., Mohler, O., Linke, C., and Schurath, U.: Measurement of wavelength-resolved light absorption by aerosols utilizing a uv-vis extinction cell, *Aerosol Sci. Tech.*, 39, 249–260, 2005.
- 20 Schwartz, S. E., Charlson, R. J., Kahn, R. A., Ogren, J. A., and Rodhe, H.: Why hasn't earth warmed as much as expected?, *J. Climate*, 23, 2453–2464, doi:10.1175/2009jcli3461.1, 2010.
- Sheridan, P. J., Arnott, W. P., Ogren, J. A., Andrews, E., Atkinson, D. B., Covert, D. S., Moosmüller, H., Petzold, A., Schmid, B., Strawa, A. W., Varma, R., and Virkkula, A.: The Reno Aerosol Optics Study: an evaluation of aerosol absorption measurement methods, *Aerosol Sci. Tech.*, 39, 1–16, 2005.
- 25 Strawa, A. W., Castaneda, R., Owano, T., Baer, D. S., and Paldus, B. A.: The measurement of aerosol optical properties using continuous wave cavity ring-down techniques, *J. Atmos. Ocean. Tech.*, 20, 454–465, 2003.
- 30 Virkkula, A.: Correction of the calibration of the 3-wavelength particle soot absorption photometer (3λ PSAP), *Aerosol Sci. Tech.*, 44, 706–712, doi:10.1080/02786826.2010.482110, 2010.

Virkkula, A., Ahlquist, N. C., Covert, D. S., Arnott, W. P., Sheridan, P. J., Quinn, P. K., and Coffman, D. J.: Modification, calibration and a field test of an instrument for measuring light absorption by particles, *Aerosol Sci. Tech.*, 39, 68–83, 2005.

5 Yu, Z., Ziemba, L. D., Onasch, T. B., Herndon, S. C., Albo, S. E., Miake-Lye, R., Anderson, B. E., Keabian, P. L., and Freedman, A.: Direct measurement of aircraft engine soot emissions using a cavity-attenuated phase shift (CAPS)-based extinction monitor, *Aerosol Sci. Tech.*, 45, 1319–1325, doi:10.1080/02786826.2011.592873, 2011.

AMTD

5, 7587–7618, 2012

Intercomparison of CAPS PM_{ex} with an Integrating Nephelometer/PSAP

A. Petzold et al.

Title Page

Abstract Introduction

Conclusions References

Tables Figures

⏪ ⏩

◀ ▶

Back Close

Full Screen / Esc

Printer-friendly Version

Interactive Discussion



Intercomparison of CAPS PM_{ex} with an Integrating Nephelometer/PSAP

A. Petzold et al.

Table 1. Instruments used during the evaluation experiments.

Instrument and manufacturer	Acronym	Property	Wavelength, nm	Time resolution	Flow, l min ⁻¹	Reference
Cavity Attenuated Phase Shift Aerodyne Res. Inc., USA	CAPS PM _{ex}	extinction	630	1 s	1.0	Massoli et al. (2010)
3λ-Integrating Nephelometer TSI Model 3563, USA	NEPH	scattering	450, 550, 700	10 s	11.0	Anderson and Ogren (1998)
3λ-Particle Soot Absorption Photometer Radiance Research Inc., USA	PSAP	absorption	467, 530, 660	1 s	0.95	Bond et al. (1999); Virkkula et al. (2005)
Multi-Angle Absorption Photometer Thermo Model 5012, USA	MAAP	absorption	637	60 s	8.0	Petzold and Schönlinner (2004); Müller et al. (2011)
Optical Particle Counter GRIMM Model 1.129, Germany	OPC	size distribution	670	6 s	1.2	

Title Page

Abstract

Introduction

Conclusions

References

Tables

Figures

⏪

⏩

◀

▶

Back

Close

Full Screen / Esc

Printer-friendly Version

Interactive Discussion

Intercomparison of CAPS PM_{ex} with an Integrating Nephelometer/PSAP

A. Petzold et al.

Table 2. Data used for the pathlength adjustment of CAPS PM_{ex}^a.

PSL		Sequence		Mie – monodisperse			Parameter of normalized PSL size distribution						Mie – polydisperse			CAPS PM _{ex}	
$d_{p, \text{nom}}$, nm		N_{total} , cm ⁻³		$C_{\text{ext}, \text{mono}}$, 10 ⁻³ cm ²	$\sigma_{\text{ep}, \text{mono}}$, M m ⁻¹		log-normal mode 1			log-normal mode 2			$C_{\text{ext}, \text{poly}}$, 10 ⁻³ cm ²	$\sigma_{\text{ep}, \text{poly}}$, M m ⁻¹		σ_{ep} , M m ⁻¹	
mean	1- σ	mean	1- σ		mean	1- σ	N_1	d_{g1} , μm	σ_{g1}	N_2	d_{g2} , μm	σ_{g2}		mean	1- σ	mean	1- σ
499	5	202	3.2	6.67	134.8	2.1	0.998	0.490	1.1	0.002	0.800	1.25	6.45	130.4	2.0	117	0.7
499	5	86	0.5	6.67	57.3	0.3							6.45	55.4	0.3	51	0.2
499	5	47	0.9	6.67	31.4	0.6							6.45	30.4	0.6	28	0.2
350	7	1669	14.6	1.76	293.5	2.6	0.981	0.350	1.1	0.019	0.460	1.15	1.92	320.5	2.8	315	1.4
350	7	928	10.4	1.76	163.1	1.8							1.92	178.1	2.0	167	0.9
350	7	523	4.0	1.76	92.0	0.7							1.92	100.5	0.8	95	0.4
903	9	48	0.3	22.0	105.9	0.7	1.000	0.850	1.2	0.000	1.0	1.2	20.6	99.2	0.7	90	0.4
903	9	27	0.3	22.0	58.8	0.7							20.6	55.0	0.7	52	0.4
701	6	214	2.1	17.4	372.7	3.6	0.813	0.62	1.1	0.188	0.85	1.2	14.1	301.5	2.9	330	1.4
701	6	103	0.6	17.4	179.0	1.1							14.1	144.8	0.9	161	0.6
701	6	50	0.5	17.4	87.5	0.8							14.1	70.8	0.6	81	0.4
596	6	456	4.5	10.8	490.0	4.9	0.867	0.57	1.1	0.133	0.7	1.2	11.0	500.2	5.0	455	2.1
596	6	315	1.2	10.8	339.0	1.3							11.0	346.0	1.3	321	0.8
596	6	105	0.8	10.8	112.8	0.8							11.0	115.2	0.8	108	0.4

^a Column content from left to right: nominal diameter of the PSL standard, $d_{p, \text{nom}}$; average total number concentration of PSL spheres, N_{total} ; extinction cross section, $C_{\text{ext}, \text{mono}}$, for monodisperse PSL spheres at diameter $d_{p, \text{nom}}$; extinction coefficient calculated for monodisperse aerosol, $\sigma_{\text{ep}, \text{mono}}$; parameters of normalized bimodal log-normal PSL size distribution fits; extinction cross section, $C_{\text{ext}, \text{poly}}$, for bimodal PSL size distributions; extinction coefficient calculated for bimodal PSL distributions, $\sigma_{\text{ep}, \text{poly}}$; extinction coefficient measured by CAPS PM_{ex}, σ_{ep} . Data are reported as mean value (mean) and 1- σ standard deviation of the mean.

Title Page

Abstract

Introduction

Conclusions

References

Tables

Figures

⏪

⏩

◀

▶

Back

Close

Full Screen / Esc

Printer-friendly Version

Interactive Discussion



Intercomparison of CAPS PM_{ex} with an Integrating Nephelometer/PSAP

A. Petzold et al.

Title Page

Abstract

Introduction

Conclusions

References

Tables

Figures

◀

▶

◀

▶

Back

Close

Full Screen / Esc

Printer-friendly Version

Interactive Discussion



Table 3. Data used for the evaluation of CAPS PM_{ex} with laboratory generated polydisperse test aerosols: AS, BC, and mixed AS + BC^a.

Run ID	Sequence time	NEPH correction ^b	σ_{ep} (630 nm) ^c		Ext. Ångström (467/630) mean	ω_0 (630 nm) mean	σ_{ep} (630 nm) ^d		CAPS PM _{ex} /NEPH-PSAP
			NEPH-PSAP mean	1- σ			CAPS PM _{ex} 1- σ		
AS1	14:06–14:34	AO98	685	1.0	2.07	1.010	709	0.3	1.03
AS2	14:45–15:00	AO98	277	0.5	2.23	1.012	294	0.2	1.06
AS3	15:23–15:36	AO98	205	0.4	2.11	1.013	224	0.1	1.09
AS4	15:50–16:10	AO98	44	0.2	1.53	1.015	50	0.1	1.13
AS5	16:20–16:40	AO98	94	0.2	1.50	1.014	107	0.1	1.14
BC1	10:18–10:26	MA09	431	1.8	0.95	0.349	404	0.9	0.94
BC2	10:30–10:35:30	MA09	379	1.5	0.97	0.349	357	0.8	0.94
BC3	10:49–11:04	MA09	84	0.3	1.02	0.360	83	0.2	0.99
BC4	11:09–11:24	MA09	31	0.4	1.03	0.344	29	0.1	0.94
MIX1	11:37–11:51	AO98	73	0.2	2.66	0.811	71	0.1	0.97
MIX2	11:59–12:14	AO98	109	0.8	2.96	0.889	106	1.0	0.97
MIX3	12:24–12:35	AO98	287	0.7	2.98	0.957	288	0.4	1.00

^a σ_{ep} data are reported as mean value (mean) and 1- σ standard deviation of the mean, averaged over the sequences of constant σ_{ep} ; all data refer to NEPH temperature and pressure conditions.

^b NEPH correction schemes: AO98 = Anderson and Ogren (1998); MA09 = Massoli et al. (2009).

^c NEPH-PSAP data were adjusted for a wavelength of 630 nm by applying the measured extinction Ångström exponent.

^d CAPS PM_{ex} data were multiplied by the pathlength adjustment factor 1.05.

**Intercomparison of
CAPS PM_{ex} with an
Integrating
Nephelometer/PSAP**

A. Petzold et al.

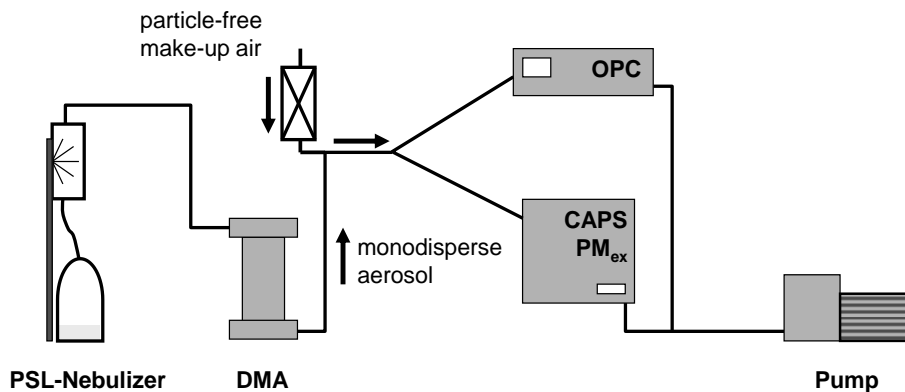


Fig. 1. Experimental set-up for the pathlength adjustment of the CAPS PM_{ex} with monodisperse PSL spheres.

[Title Page](#)[Abstract](#)[Introduction](#)[Conclusions](#)[References](#)[Tables](#)[Figures](#)[⏪](#)[⏩](#)[◀](#)[▶](#)[Back](#)[Close](#)[Full Screen / Esc](#)[Printer-friendly Version](#)[Interactive Discussion](#)

Intercomparison of CAPS PM_{ex} with an Integrating Nephelometer/PSAP

A. Petzold et al.

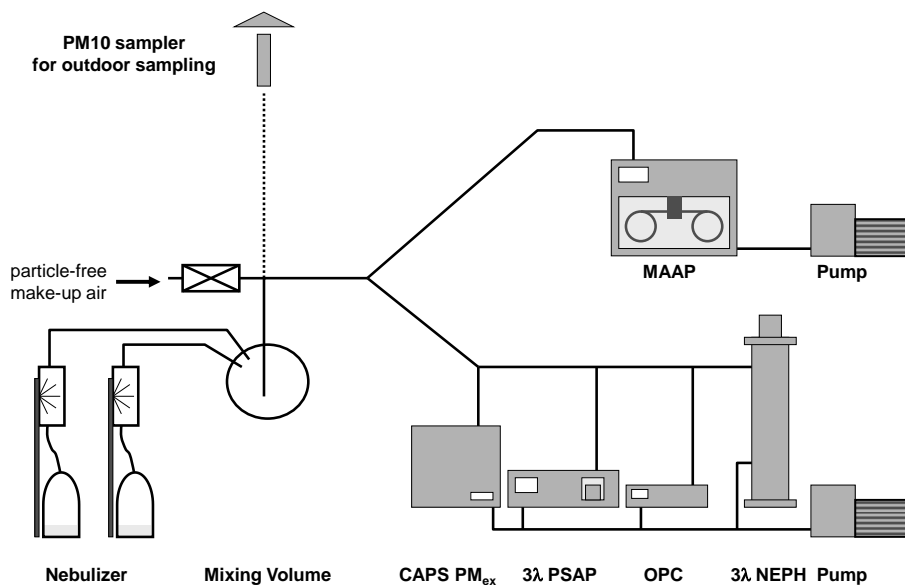


Fig. 2. Experimental set-up for the instrument evaluation using polydisperse aerosol mixtures of black carbon and ammonium sulfate; the sampling line was switched to the outdoor PM₁₀ sampler (dashed line), for measuring ambient aerosol.

Title Page	
Abstract	Introduction
Conclusions	References
Tables	Figures
⏪	⏩
⏴	⏵
Back	Close
Full Screen / Esc	
Printer-friendly Version	
Interactive Discussion	

Intercomparison of CAPS PM_{ex} with an Integrating Nephelometer/PSAP

A. Petzold et al.

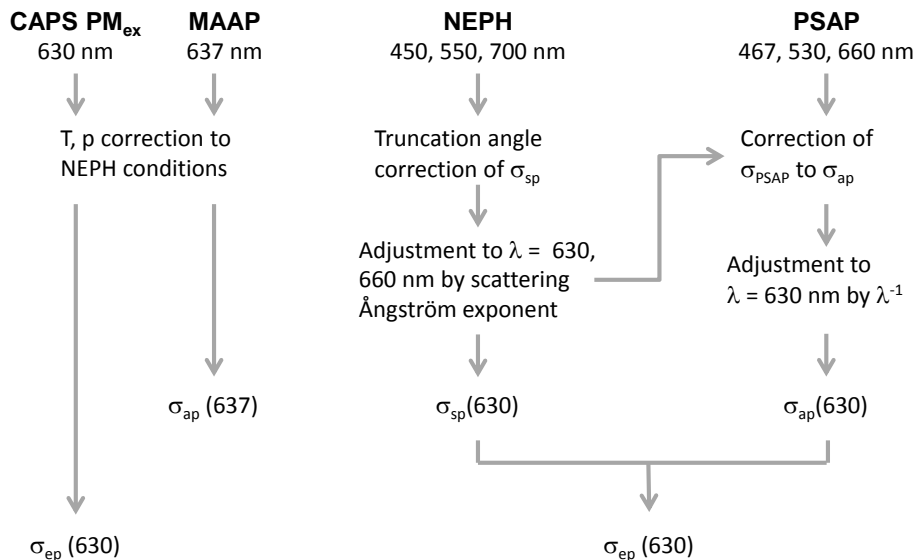


Fig. 3. Schematic of the data inversion procedures for the optical instruments.

Title Page

Abstract

Introduction

Conclusions

References

Tables

Figures

◀

▶

◀

▶

Back

Close

Full Screen / Esc

Printer-friendly Version

Interactive Discussion



**Intercomparison of
CAPS PM_{ex} with an
Integrating
Nephelometer/PSAP**

A. Petzold et al.

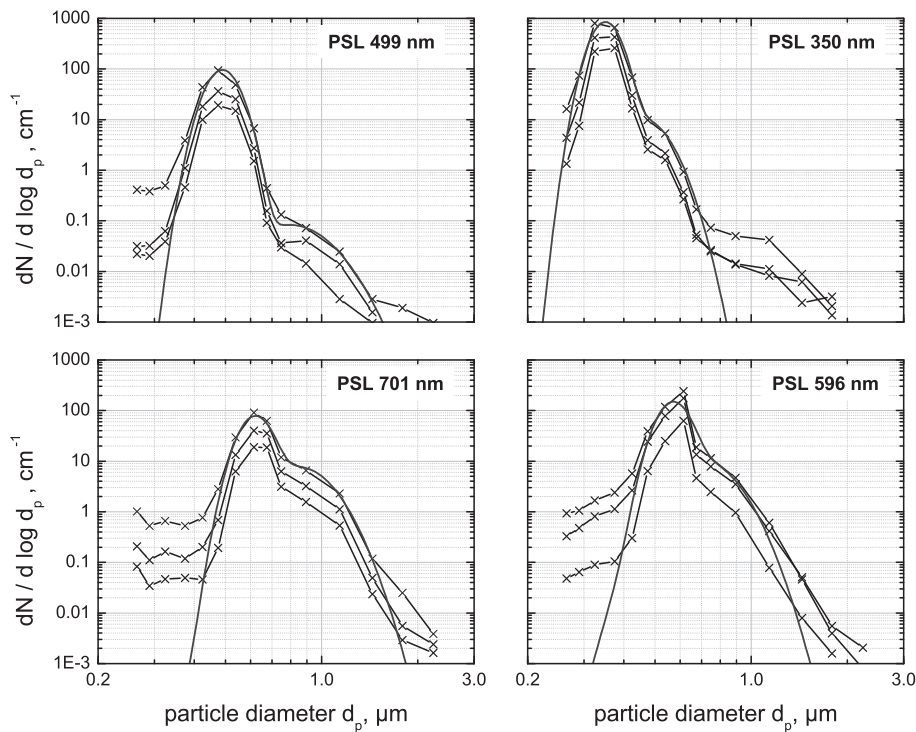


Fig. 4. Number size distributions of PSL spheres measured downstream of the DMA; grey lines represent bimodal log-normal size distributions representing PSL and PSL conglomerates. Nominal sizes of atomized PSL standards are indicated.

[Title Page](#)[Abstract](#)[Introduction](#)[Conclusions](#)[References](#)[Tables](#)[Figures](#)[◀](#)[▶](#)[◀](#)[▶](#)[Back](#)[Close](#)[Full Screen / Esc](#)[Printer-friendly Version](#)[Interactive Discussion](#)

Intercomparison of CAPS PM_{ex} with an Integrating Nephelometer/PSAP

A. Petzold et al.

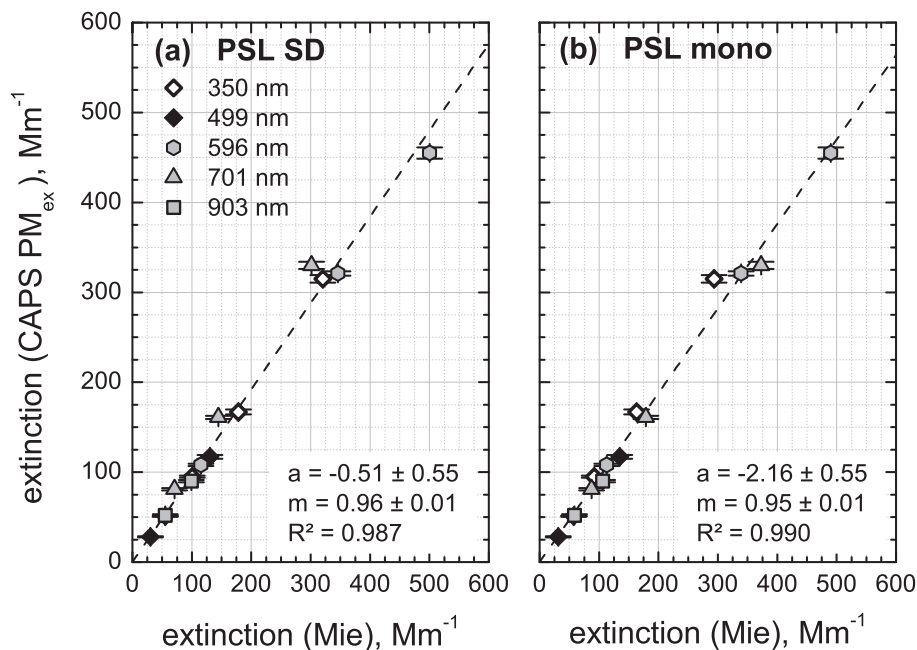


Fig. 5. Comparison of extinction at a wavelength of 630 nm measured by the CAPS PM_{ex} instrument (y-axis) and extinction calculated for PSL spheres using the full size distribution information **(a)** and assuming monodisperse spheres at the nominal diameter **(b)**.

[Title Page](#)
[Abstract](#)
[Introduction](#)
[Conclusions](#)
[References](#)
[Tables](#)
[Figures](#)
[⏪](#)
[⏩](#)
[◀](#)
[▶](#)
[Back](#)
[Close](#)
[Full Screen / Esc](#)
[Printer-friendly Version](#)
[Interactive Discussion](#)

**Intercomparison of
CAPS PM_{ex} with an
Integrating
Nephelometer/PSAP**

A. Petzold et al.

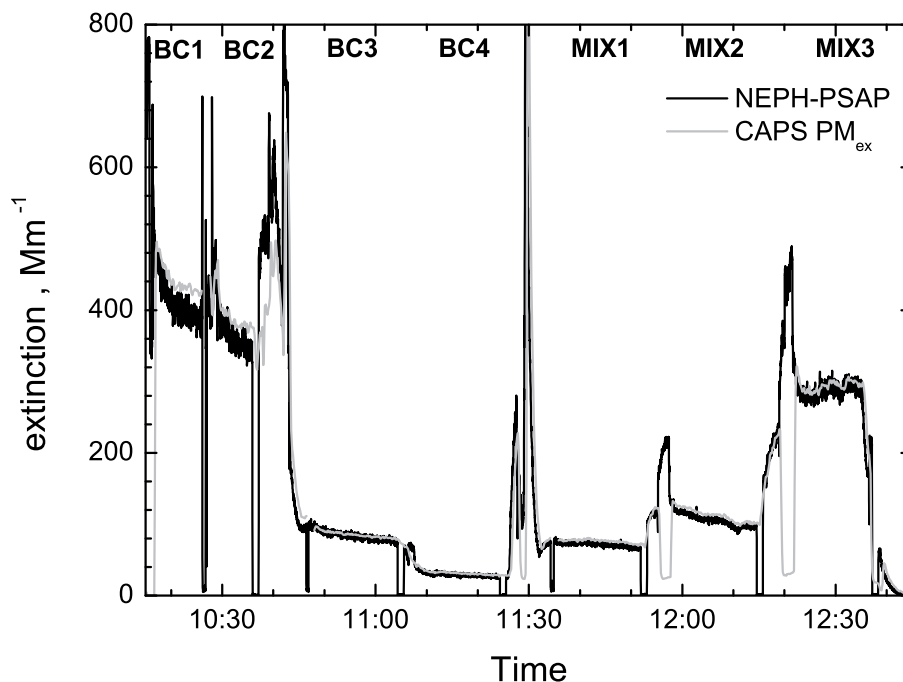


Fig. 6. Time series of CAPS PM_{ex} extinction (black) and NEPH-PSAP extinction (grey) for the laboratory generated polydisperse BC and mixed AS + BC experiments; analyzed sequences are labeled at the top x-axis.

[Title Page](#)[Abstract](#)[Introduction](#)[Conclusions](#)[References](#)[Tables](#)[Figures](#)[⏪](#)[⏩](#)[◀](#)[▶](#)[Back](#)[Close](#)[Full Screen / Esc](#)[Printer-friendly Version](#)[Interactive Discussion](#)

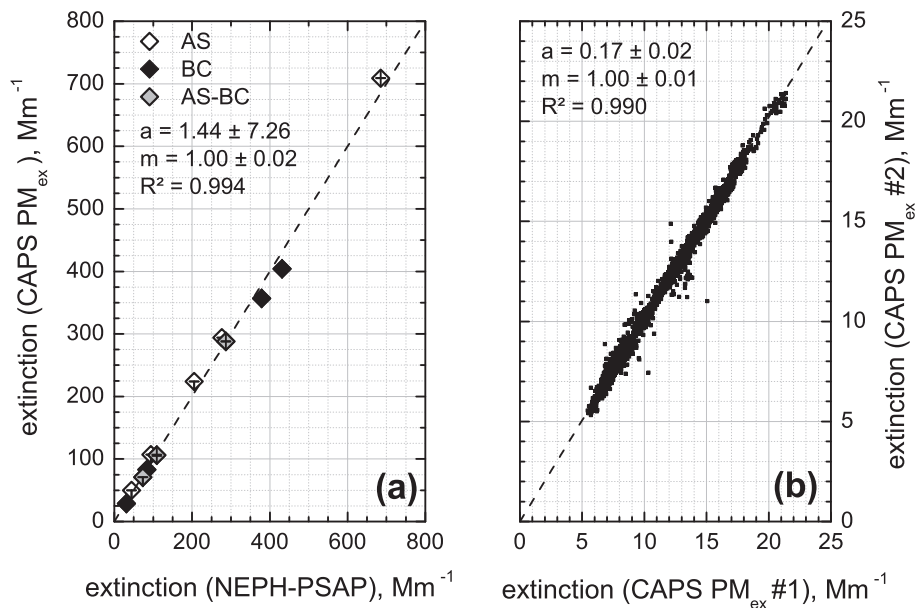


Fig. 7. (a) Accuracy: Intercomparison of extinction measured by CAPS PM_{ex} and extinction obtained from the combined NEPH-PSAP analysis for polydisperse laboratory aerosols; all data refer to a wavelength of 630 nm. (b) Precision: intercomparison of two CAPS PM_{ex} monitors operated side-by-side while sampling from ambient aerosol with 15 s time resolution. The dashed lines represent the 1 : 1 ratio.

Intercomparison of CAPS PM_{ex} with an Integrating Nephelometer/PSAP

A. Petzold et al.

Title Page

Abstract

Introduction

Conclusions

References

Tables

Figures

⏪

⏩

◀

▶

Back

Close

Full Screen / Esc

Printer-friendly Version

Interactive Discussion

**Intercomparison of
CAPS PM_{ex} with an
Integrating
Nephelometer/PSAP**

A. Petzold et al.

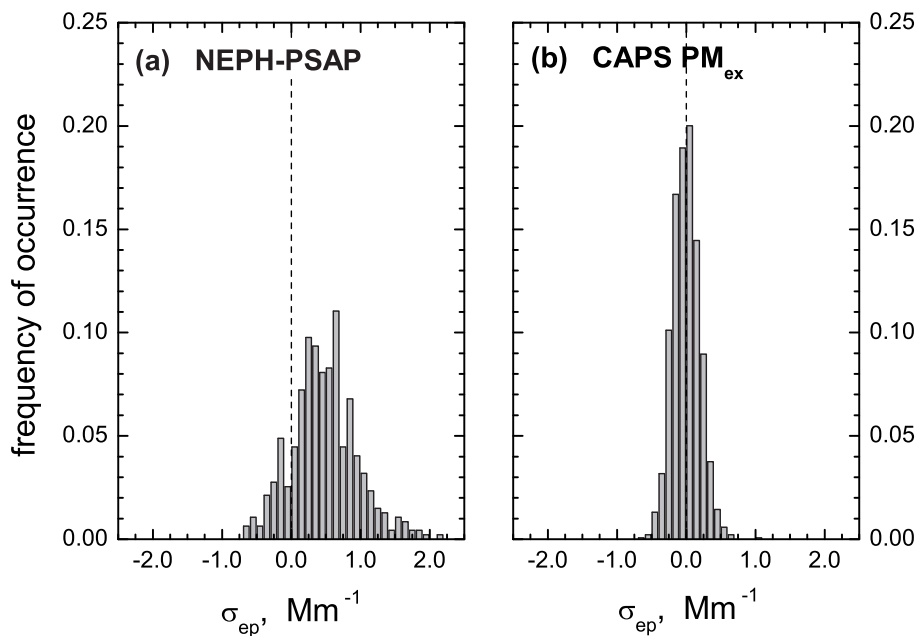


Fig. 8. Histograms of the electronic noise of NEPH-PSAP (left panel) and CAPS PM_{ex} (right panel) averaged for > 1 h of sampling particle-free air.

[Title Page](#)[Abstract](#)[Introduction](#)[Conclusions](#)[References](#)[Tables](#)[Figures](#)[⏪](#)[⏩](#)[◀](#)[▶](#)[Back](#)[Close](#)[Full Screen / Esc](#)[Printer-friendly Version](#)[Interactive Discussion](#)

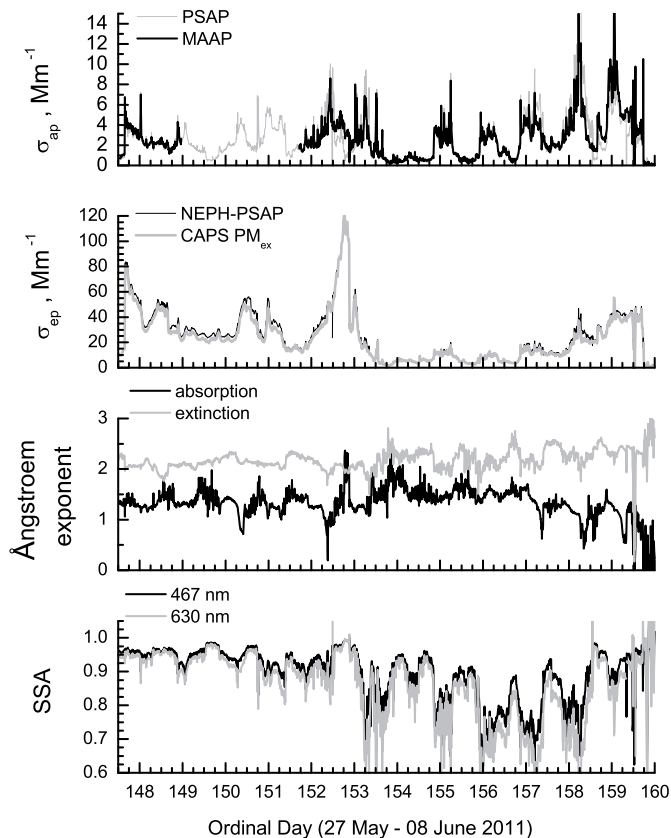


Fig. 9. Time series of aerosol optical properties at $\lambda = 630$ nm measured for ambient aerosol at Aerodyne Research Inc. premises. Properties are absorption coefficient, σ_{ap} , from MAAAP and PSAP; extinction coefficient, σ_{ep} , from CAPS PM_{ex} and NEPH-PSAP; Ångström exponents of extinction and absorption for the wavelength ratio 467/630 nm; and single-scattering albedo, SSA, for wavelengths 467 and 630 nm.

Intercomparison of CAPS PM_{ex} with an Integrating Nephelometer/PSAP

A. Petzold et al.

Title Page

Abstract Introduction

Conclusions References

Tables Figures

◀ ▶

◀ ▶

Back Close

Full Screen / Esc

Printer-friendly Version

Interactive Discussion



**Intercomparison of
CAPS PM_{ex} with an
Integrating
Nephelometer/PSAP**

A. Petzold et al.

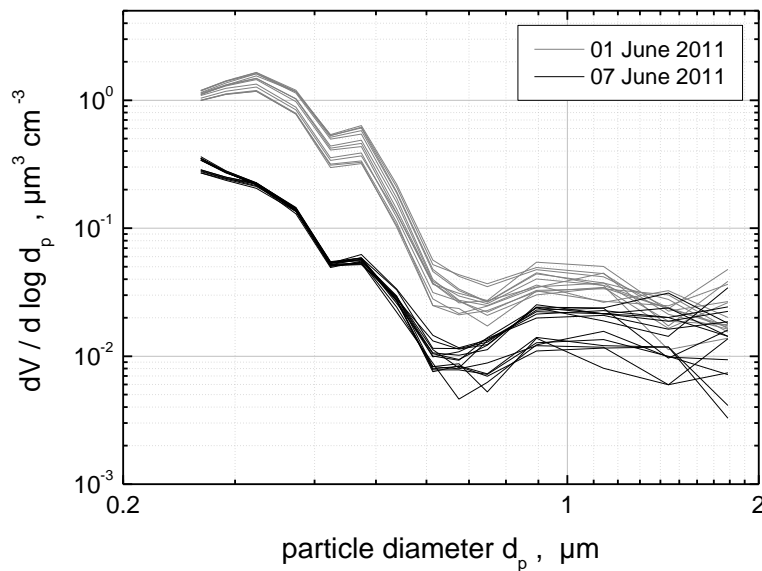


Fig. 10. Volume size distributions for 1 June (high pollution sequence; ordinal day 152) and 7 June (moderate pollution sequence; ordinal day 158) calculated from OPC size distributions.

[Title Page](#)[Abstract](#)[Introduction](#)[Conclusions](#)[References](#)[Tables](#)[Figures](#)[◀](#)[▶](#)[◀](#)[▶](#)[Back](#)[Close](#)[Full Screen / Esc](#)[Printer-friendly Version](#)[Interactive Discussion](#)

**Intercomparison of
CAPS PM_{ex} with an
Integrating
Nephelometer/PSAP**

A. Petzold et al.

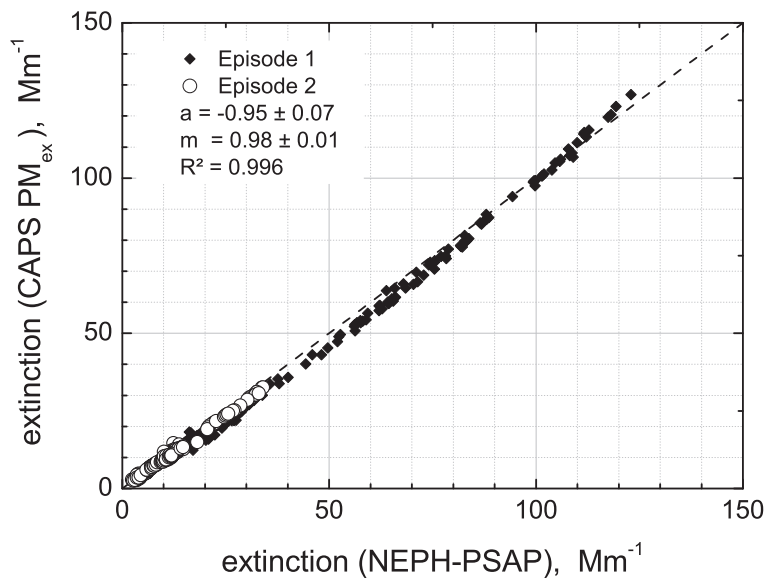


Fig. 11. Intercomparison of extinction measured by CAPS PM_{ex} and extinction obtained from the combined NEPH-PSAP analysis for ambient aerosols; the dashed line represents the 1 : 1 relation.

[Title Page](#)[Abstract](#)[Introduction](#)[Conclusions](#)[References](#)[Tables](#)[Figures](#)[◀](#)[▶](#)[◀](#)[▶](#)[Back](#)[Close](#)[Full Screen / Esc](#)[Printer-friendly Version](#)[Interactive Discussion](#)

**Intercomparison of
CAPS PM_{ex} with an
Integrating
Nephelometer/PSAP**

A. Petzold et al.

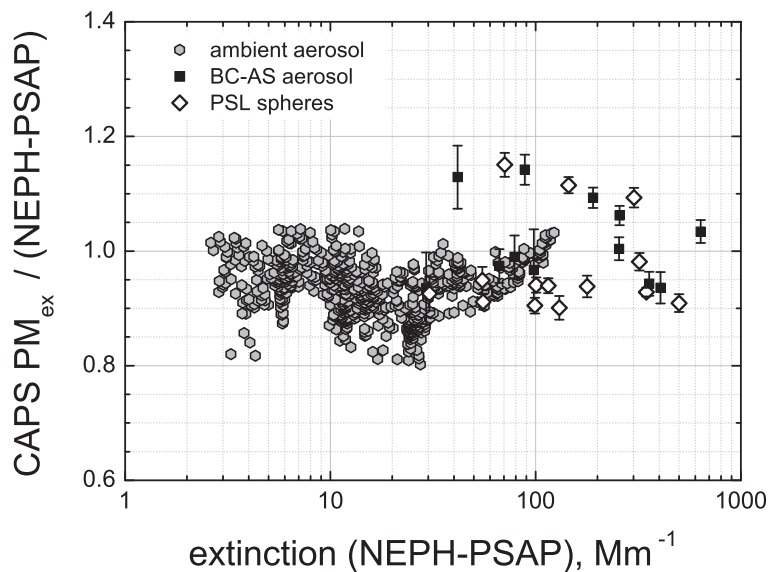


Fig. 12. Ratio of extinction reported by CAPS PM_{ex} to extinction calculated from NEPH-PSAP for the entire range of extinction coefficients measured for laboratory and ambient aerosols; ambient aerosol data are 10 min average values.

[Title Page](#)[Abstract](#)[Introduction](#)[Conclusions](#)[References](#)[Tables](#)[Figures](#)[⏪](#)[⏩](#)[◀](#)[▶](#)[Back](#)[Close](#)[Full Screen / Esc](#)[Printer-friendly Version](#)[Interactive Discussion](#)